

HYDROCARBONS IN THE UPPER PERMIAN PZ1–PZ2 CYCLES OF THE KŁODAWA SALT STRUCTURE, CENTRAL POLAND

Łukasz WOLNY¹, Franciszek CZECHOWSKI¹, Stanisław BURLIGA¹,
Paweł RACZYŃSKI¹ & Marek HOJNIAK²

¹*University of Wrocław, Institute of Geological Sciences; pl. M. Borna 9, 50-204 Wrocław, Poland; lukasz.wolny@ing.uni.wroc.pl, franciszek.czechowski@ing.uni.wroc.pl, stanislaw.burliga@ing.uni.wroc.pl, pawel.raczynski@ing.uni.wroc.pl*

²*University of Wrocław, Faculty of Chemistry; F. Joliot-Curie 14, 50-383 Wrocław, Poland; marek.hojniak@chem.uni.wroc.pl*

Wolny, Ł., Czechowski, F., Burliga, S., Raczyński, P. & Hojniak, J., 2014. Hydrocarbons in the Upper Permian PZ1–PZ2 cycles of the Kłodawa Salt Structure, central Poland. *Annales Societatis Geologorum Poloniae*, 84: 363–374.

Abstract: Organic geochemical studies were carried out on the sulphate–shale–carbonate series, representing the upper PZ1 and lower PZ2 sections of the Zechstein cycles in the Kłodawa Salt Structure, located in the central part of the Zechstein Basin, in Poland. Hydrocarbons extracted from the Na1 and Na2 rock salts, the A1g and A2 anhydrites, the Ca2 dolomitic anhydrite and the T2 shale-carbonate rocks were analysed by gas chromatography mass spectrometry (GC-MS). Homological series of the *n*-alkanes and chained isoprenes indicate the algal nature of the organic matter with the characteristic chemistry of type II kerogen deposited under anoxic conditions. The molecular composition of other biomarkers (*n*-alkylbenzenes, steranes) as well as phenanthrene and dibenzothio-*phene* and their methyl derivatives revealed the highest maturity of the hydrocarbons (level of advanced stage of the oil-window zone) in the upper part of the Stinking Shale. In the adjacent beds, a gradual decrease in the maturity of the hydrocarbons was observed both upwards and downwards in the stratigraphic sequence. The main source rock of the hydrocarbons is represented by the Stinking Shale deposits. The observed trend of vertical variation in maturity through the rock profile is explained as resulting from the continuous vertical migration of hydrocarbons, expelled during maturation from the Stinking Shale rocks into the underlying and overlying strata.

Key words: Zechstein Basin, Kłodawa Salt Structure, PZ1–PZ2 rocks, hydrocarbons, biomarkers, maturity, hydrocarbons migration.

Manuscript received 19 February 2014, accepted 8 December 2014

INTRODUCTION

Evaporite sequences provide both seals and traps for hydrocarbon accumulation in many sedimentary basins, particularly where rock salt with very low permeability occurs in an evaporite series (Warren, 1999; Sarg, 2001). Rock salt most commonly acts as a cap rock, which prevents both the infiltration of hydrocarbons into the overlying strata and the inflow of ground water into the reservoir rocks. If the reservoir rocks are located between rock salt layers, they become inaccessible for fluids, circulating outside the rock salt body. In the Upper Permian (Zechstein) carbonate-evaporite sequences of central Europe, the majority of liquid hydrocarbon accumulations occur in carbonates of the second evaporitic cycle (PZ2), referred to as the Main Dolomite (Ca2). These deposits occur within a sequence of sulphate-shale-carbonate-sulphate rocks, which separate thick rock salt beds of the first (PZ1) and second (PZ2) evaporitic cycles. In Poland, the Ca2 deposits were studied

most thoroughly in the marginal parts of the Zechstein Basin, where oil and gas accumulations are found in carbonate platform and slope deposits (Jaworowski and Mikołajewski, 2007; Karnkowski, 2007; Kotarba and Wagner, 2007; Słowakiewicz and Mikołajewski, 2009, 2011). However, in the open basin area, organic geochemical data on the Upper Permian reservoir rocks and adjacent sulphates and shales are still fragmentary. The studies carried out in the salt diapirs of central Poland revealed that hydrocarbons also occur in deposits of the deepest part of the Zechstein Basin (Bąkowski and Tokarski, 1966; Bąkowski, 1986; Natkaniec-Nowak *et al.*, 2001; Burliga *et al.*, 2008). Since the Ca2 deposits were not evidenced conclusively in the salt structures, the early investigations were mainly focused on analyses of bituminous rock salt and oil seepages in salt mines. Those geochemical studies on the PZ1–PZ2 rock complex (Natkaniec-Nowak *et al.*, 2001; Toboła, 2010) were carried out on randomly selected rock samples, for which stratigraphic correlation to the Zechstein series was difficult. Recent studies

revealed the local occurrence of Ca₂ strata as blocks in the Kłodawa Salt Structure. In particular, geochemical analyses of these Ca₂ blocks permitted determination of hydrocarbons maturity in the potential reservoir rocks on a peak-oil-window stage (Czechowski *et al.*, 2011). The preliminary analyses were performed on selected samples from the Main Dolomite and the Stinking Shale, found in the 15a Mine Gallery, as well as on migrated hydrocarbons with coal-like material, filling fractures in the profile (Czechowski *et al.*, 2011; Wagner and Burliga, 2014).

The present account extends these preliminary findings and presents new data on the molecular composition of the hydrocarbons, trapped in a boudin that is composed of the complete carbonate–evaporite–siliciclastic rock sequence, located in the 18a Mine Gallery. This sequence, located approximately 100 m north of the 15a Mine Gallery, originally separated the Oldest Halite (PZ1) and the Older Halite (PZ2) rock salt beds and does not contain any fractures, filled with hydrocarbons that might have migrated there. Owing to the isolation of the strata in impermeable rock salt, it is assumed that the organic geochemical characteristics of these rocks are representative for the primary Zechstein deposits, with no imprint of organic matter from the surrounding deposits. The aims of the study were to recognize the environmental conditions during deposition of both the evaporite and shale beds as well as to assess the genetic type of the hydrocarbons sources and their maturity, on the basis of biomarker indices.

GEOLOGICAL SETTING

The Kłodawa Salt Structure (KSS) is a diapiric ridge, composed of Upper Permian (Zechstein) evaporite–siliciclastic rocks, which originally constituted a marine sedimentary sequence, deposited in the central part of the Polish Zechstein Basin (Fig. 1), a subbasin situated in the eastern part of the Southern Permian Basin (Ziegler, 1990; Wagner, 1994; Kotarba *et al.*, 2006; Peryt *et al.*, 2010). Four sedimentary sequences are distinguished in the basin fill, annotated as the PZ1 (Werra), PZ2 (Stassfurt), PZ3 (Leine) and PZ4 (Aller) cycles (Wagner, 1994). The analysis of tectonic structures inside the diapir revealed that the deformation of the Zechstein sequence started in (sub)horizontally arranged beds in the early Triassic (Burliga, 1996a, 1996b), whereas the regional seismic sections (Krzywiec, 2004) indicate that the Zechstein rocks diapirically pierced through their cover as early as in the late Triassic. The seismic sections also imply repetitive burial and reactivation of the vertical rise of the KSS during the Jurassic and Cretaceous. Therefore, the top of the KSS in the study area remained shallowly buried during that time interval. During the latest Cretaceous (Maastrichtian)–early Paleogene, the basin was inverted and the topography in the KSS area was levelled by erosion and subsequently covered by Cenozoic deposits (Dadlez *et al.*, 1995; Dadlez, 2003; Krzywiec, 2006a, b; Jarosiński *et al.*, 2009; Krzywiec *et al.*, 2009). The thickness of the Cenozoic cover varies in the range of about 100–200 m above the shallowly buried sections of the KSS and the Zechstein source layer is about 6 km below the surface, at present.

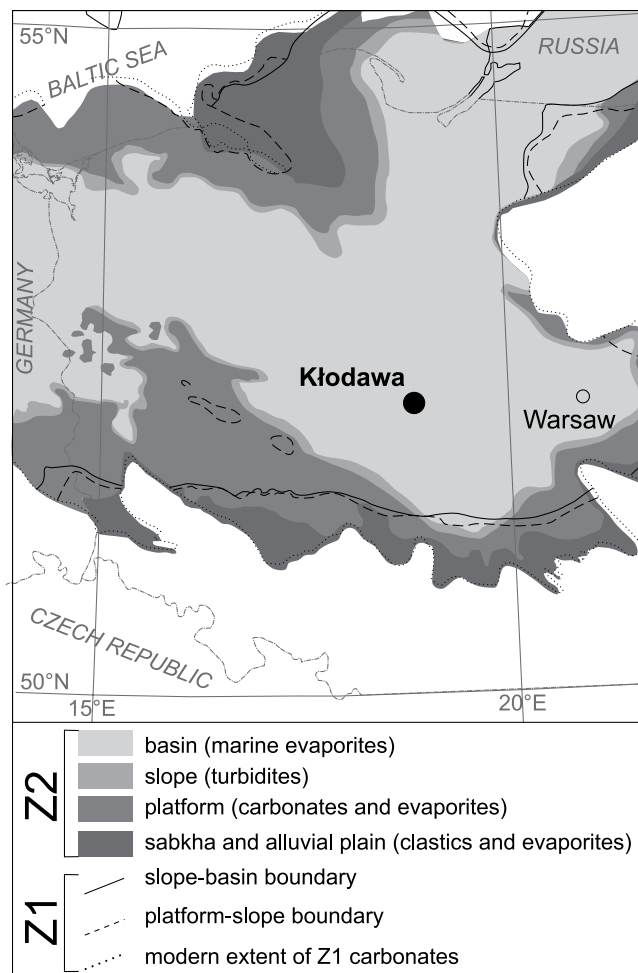


Fig. 1. Location of the Kłodawa Salt Structure (“Kłodawa SA” salt mine) on generalized map of Southern Permian Basin extent in territory of Poland (map after Peryt *et al.*, 2010).

The rock salt beds of the PZ1 and PZ2 cycles are separated vertically by bedded deposits of the Upper Anhydrite (A1g), the Stinking Shale (T2), the Main Dolomite (Ca₂) and the Basal Anhydrite (A2), representing a transgressive systems tract and highstand systems tract (TST–HST) complex (Peryt and Wagner, 1998; Kovalevych *et al.*, 2008). The palaeogeography and facies distribution in the central part of the Zechstein Basin during A1g–A2 sedimentation are poorly recognized, since the deposits are deeply buried (4–7 km) and were penetrated by very few boreholes. On the basis of facies patterns in the marginal parts of the basin, it is inferred that the KSS developed on a basin plain (Fig. 1; compare Wagner, 1994; Słowakiewicz and Mikołajewski, 2011). The only geological data on the lithology, stratigraphy and thickness of the A1g–A2 complex in the deepest part of the Zechstein Basin derive from a few diapiric salt structures, in which salt-mine excavations cut across Zechstein deposits. However, owing to the higher competence of the A1g–A2 rocks (sulphate, carbonate and clay rocks) by comparison with the rock salt, these competent beds became intensively boudinaged and brecciated during salt flow. They mostly are preserved as irregular blocks of anhydrite, randomly dispersed in rock salt (Burliga *et al.*, 2008). As a result, published data on the

lithology of the A1g-A2 complex are extremely poor (e.g., Kucia, 1970; Misiek, 1997). A continuous, well-preserved sedimentary sequence of A1g-A2 deposits was established only recently (Czechowski *et al.*, 2011). These bedded deposits constitute a large-scale boudin, which is completely surrounded by rock salt. The boudin extends sub-vertically for a distance of over 100 m in its maximum dimensions, both horizontally and vertically. In the study area, the total thickness of the A1g-A2 beds is about 23.8 m. Weak deformation of the beds and the continuity of the sedimentary succession indicate boudin isolation by the rock salt at a very early stage in the deformation of the evaporite series and it floated as a raft in a salt mass during the uplift of the KSS. In the context of the overall evolution of the KSS, this boudin was isolated by the salt, most probably since the Early Triassic.

MATERIALS AND METHODS

Rock samples

The samples investigated are from the only accessible A1g-A2 section that is complete; it is located in the KS 18a Mine Gallery, at a depth of 650 m. They were collected from the gallery wall and ceiling, away from any rock fractures. The sampled section included strata from the Oldest Halite through the Upper Anhydrite, the Stinking Shale, the Main Dolomite, and the Basal Anhydrite, up to the Older Halite. The sampling sites and their annotation are given in Fig. 2.

The A1g-A2 series are distinctly layered and with the exception of the top of the Main Dolomite bed, the boundaries between the lithostratigraphic units and beds are sharp. The Main Dolomite bed is made up of dolomitic anhydrite and therefore the contact between the Ca2 and A2 deposits is gradational and indistinct. Owing to the indistinct nature of the upper boundary, the estimated thickness of the Main Dolomite bed is in the range of 20–30 cm. The Na1 and Na2 beds are rock salts with fine, dark laminae, enriched in anhydrite. The T2 bed is dominantly composed of carbonate and siliciclastic minerals, whereas the A1g and A2 beds are anhydrite. The above observations strongly support the view that the profile analysed represents a continuous, weakly deformed sequence of PZ1 and PZ2 deposits.

Uncovered thin sections for all of the rock types, except halite, were prepared by trimming down rock slices attached to glass slides by means of epoxy, until the samples were 30 μm thick. The samples obtained in this way were analysed, using an optical microscope equipped with cathodoluminescence. The microscopic mineralogical observations of the samples were confirmed by XRD analyses (Siemens D-5005, Bragg angles used to collect the x-ray data from 10 to 75 degree).

Extraction of hydrocarbons

Finely powdered rock samples of mass about 100 g were placed in pre-extracted thimbles, and extracted, using the Soxhlet apparatus (until the disappearance of the pale luminescence, observed under UV light, which lasted about two days) with a mixture of azeotropic dichloromethane and methanol (volumetric proportions 93:7 v/v, respectively).

From the extracts obtained, the solvent was evaporated on a rotary evaporator at a bath temperature of 40 °C to obtain 0.5 mL of concentrated aliquots. They consisted of residual solvent and mainly light hydrocarbons. Owing to the low yields of extracts and the need to preserve compounds of low molecular weight in the extracts, the aliquots obtained were not further fractionated by the TLC. Therefore, the quantitative assessment of the extracts was arbitrary. The analysis of concentrated aliquots was performed by using gas chromatography–mass spectrometry (GC-MS).

Gas chromatography–mass spectrometry

The GC-MS analysis of the total extracts was carried out with a HP5890 II gas chromatograph, equipped with a HP-5 fused silica capillary column (30 m x 0.25 mm i.d., coated with 5% diphenylpolysiloxane and 95% dimethylsiloxane phase with 0.25 μm film thickness). Helium was used as a carrier gas at a flow rate of 1 $\text{cm}^3 \text{min}^{-1}$. The GC oven was heated from 25 °C to 290 °C at a rate of 3 °C min^{-1} and kept for 30 min at the final temperature. The detection was performed by a HP 5971A mass spectrometer detector, interfaced to a gas chromatograph. The quadrupole mass spectrometer detector was operated in an electron impact mode with an ionization energy of 70 eV and an ion source temperature of 200 °C. Data were acquired in full scan mode (mass range m/z 50–600 with cycle time of 1 s). The compound groups were extracted from the total ion current (TIC) mass chromatogram, using selective fragment ions. For the mass chromatograms of the compound groups, the following fragment ions were used: free *n*-alkanoic acids (m/z 60), *n*-alkanes and chained isoprenoids (m/z 85), sesquiterpanes (m/z 123), *n*-alkylbenzenes (m/z 92), steranes (m/z 217), secosteranes (m/z 219, 233 and 247), and molecular ions for phenanthrene (m/z 178), methylphenanthrenes (m/z 192), dibenzothiophene (m/z 184) and methyl-dibenzothiophenes (m/z 198). The concentrations of other groups of compounds in the extracts were below the detection limit. Compound identification was based on literature data, the comparison of GC retention time with selected authentic standards, and the interpretation of mass spectrometric fragmentation patterns. The relative quantification of given compounds was based on integration data from the corresponding mass chromatograms.

RESULTS AND DISCUSSION

Thin-sections of the T2, Ca2 and A2 samples revealed very fine lamination within the beds and the alternation of laminae with higher and lower amounts of organic matter (Fig. 2). Observations of the A1g-3 anhydrite (Fig. 2) revealed the presence of minor admixtures of carbonates and quartz. Samples of the Stinking Shale (T2-2 and T2-3 in Fig. 2) are laminated clay-carbonate rocks with dispersed minor quartz, mica and sulphide. The carbonates consist of biogenic components (foraminiferas, ostracods, bivalves, gastropods). The Main Dolomite sample is composed mainly of anhydrite with presence of a dolomite crystals stretched in the form of lenses (Fig. 2). Fragments of fossils, most likely molluscs, are also present.

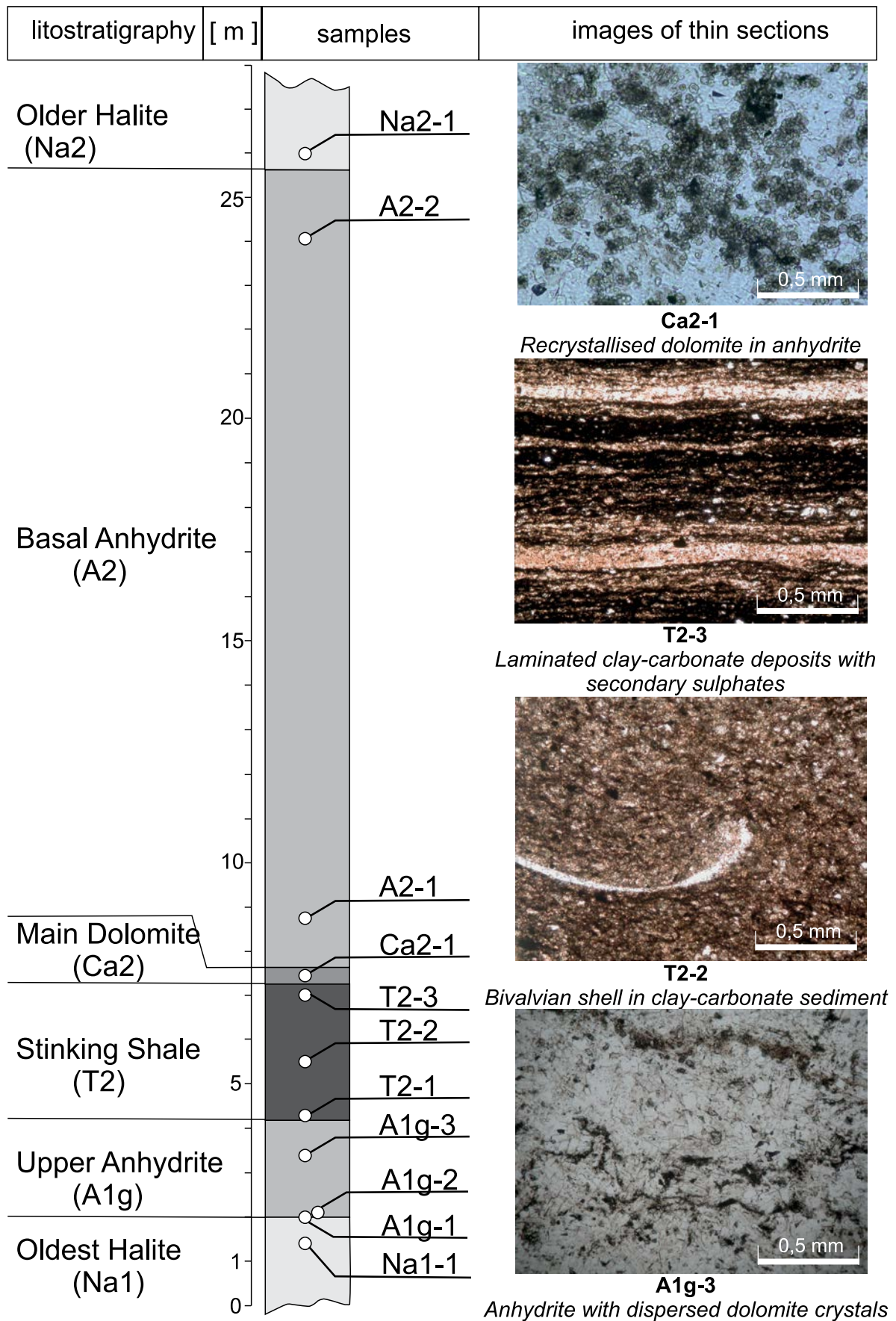


Fig. 2. Sampling sites in Zechstein PZ1–PZ2 lithostratigraphic profile located in KS 18a Mine Gallery with microscopic images of thin sections from selected samples (photograph width 1.73 mm PPL).

The hydrocarbons extracted from the rocks analysed are represented by *n*-alkanes, *n*-alkylbenzenes, acyclic C₁₃–C₂₀ isoprenoids (with pristane (Pr) and phytane (Ph) domination) as well as phenanthrene and dibenzothiophene and their polymethyl derivatives. Classical biomarkers, such as pentacyclic triterpanes (hopanes) or aryl isoprenoids were lacking in these rocks. Steranes were evidenced only in the dolomitic anhydrite. GC-MS analysis of the extract concentrates revealed very low amounts (traces) of hydrocarbons in the halite and anhydrite samples, whereas their content in the T2 and Ca2 beds as well as in the anhydrite samples from the boundaries with the Stinking Shale and the Main Dolomite (samples A1g-3 and A2-1 respectively) was estimated to be around 3–10 times higher.

Hydrocarbons composition

The variation in homological distribution of *n*-alkanes and isoprenoids, the major hydrocarbons in the rocks throughout the profile of PZ1–PZ2 stratigraphic succession described, is illustrated in Fig. 3, column a. It shows a distinct *n*-alkane fingerprint in the uppermost Stinking Shale sample (T2-3), where the relative abundance of the homologues over the range from *n*-C₁₀ to *n*-C₃₅ gradually decreases with homologue chain length (Fig. 3, trace T2-3 in column a). The *n*-alkanes in the samples collected from below and above the T2-3 bed show a monomodal, nearly gaussian homologous distribution. Furthermore, with increasing distance from the T2-3 bed the homologue with maximum abundance gradually shifts to one with a higher molecular weight (from *n*-C₁₁ to *n*-C₂₀, see Table 1). Such an upward shift of *n*-C_{max} towards homologues of higher molecular weight within the dolomite above the Kupferschiefer was observed previously by Kluska *et al.* (2013). This is also reflected in the gradually lowering of values of the *n*-C₂₁/*n*-C₂₁₊ ratio in the Ca2 dolomitic anhydrite and the A1g and A2 anhydrites (Table 1) with increasing distance from the T2 bed. In addition, in the Ca2-1 and A1g-1 samples (not illustrated in Fig. 3), a second, subordinate maximum is present, centred around *n*-C₂₆. In sample T2-3, the ratios of Pr relative to *n*-C₁₇ and Ph relative to *n*-C₁₈ (calculated from data of the integrated area of the corresponding peaks on the TIC chromatogram) are the lowest (0.41 and 0.47, respectively), indicating the highest maturity of the hydrocarbons present. A trend of increases in these values downwards and upwards within the stratigraphic sequence (excluding the weakly permeable Na1-1 and Na2-1 rock salt) indicates corresponding directions of decreasing hydrocarbon maturity. It results from maturity variation, due to the earlier expulsion of the less matured hydrocarbons at lower maturation stages from the Stinking Shale source rock and their further inflow into the underlying and also the overlying rocks (Table 1). However, the distinctly elevated Ph/*n*-C₁₈ value in Ca2-1 (1.81), much higher than that observed for the T2 strata (Table 1) as well as for the A2 samples, is indicative of a more anoxic depositional environment during Ca2 sedimentation. This discrepancy results from the mixing of hydrocarbons flowing into Ca2 from the underlying T2 source rock with those generated and accumulated

in the Ca2 source rock. Anoxic conditions are confirmed by the lower unity CPI values, indicating the prevalence of even-carbon-numbered *n*-alkanes over their odd-carbon-numbered counterparts (Bray and Evans, 1961; Hunt, 1996). This is particularly evident in the Ca2 formation in the *n*-C₂₃ – *n*-C₃₁ homologous range (Table 1). Also the value of the terrestrial/aquatic ratio (TAR parameter), introduced by Bourbonniere and Meyers (1996), is lower in the Ca2-1 sample, as compared to the value in the T2-3 sample, which are 0.21 and 0.25, respectively. A gradual increase in TAR values downwards from the T2 strata is interpreted as being a result of migration of hydrocarbons with higher molecular mass, expelled at earlier stages of maturity into the underlying strata (Table 1).

The pristane-phytane ratio (Pr/Ph) is commonly used as a redox indicator of the depositional environment (Powell and McKirdy, 1973; Didyk *et al.*, 1978; ten Haven *et al.*, 1985). Its value is also related to the salinity of the sedimentary basin. Their most common sources are the chlorophylls of phototrophic organisms (Brooks *et al.*, 1969) and the lipids of halophilic bacteria and archaea (ten Haven *et al.*, 1985; ten Haven *et al.*, 1988). The Pr/Ph ratios below unity (Table 1) are indicative of anoxic conditions during the deposition of organic matter (Didyk *et al.*, 1978; ten Haven *et al.*, 1985; Peters *et al.*, 2005). Particularly low Pr/Ph values (below <0.5) are found in the Ca2 and somewhat higher values (around 0.65) in the A1g strata, reflecting a highly anoxic and suboxic depositional environment. More elevated Pr/Ph values (around 1.0) are observed in the T2 and A2 beds as well as in the Na1 and Na2 rock salts. A Pr/Ph ratio of close to unity for the Stinking Shale deposits also was determined at another location in the Kłodawa Salt Structure (Burliga and Czechowski, 2010).

In the samples analysed, pentacyclic triterpane biomarkers (hopanes) were not detected. Their absence can result from the advanced maturity of the source rocks. A low concentration of steranes was evidenced only in the Main Dolomite. Their mass fragmentogram, illustrated in Fig. 4, shows the prevalence of C₂₉ homologues over their C₂₈ and C₂₇ counterparts (60, 22 and 18%, respectively; see Table 1), which is typical for carbonate sediments (Volkman, 1986). However, they contain diasteranes, i.e. the products of the catalytic rearrangement of steranes by accessory clay minerals. The authors suggest that the part of the steranes containing diasteranes, preserved in the Main Dolomite, are migration constituents, released at a lower maturity stage from the underlying Stinking Shale, containing much of the siliclastic material. Also the interaction of hydrocarbons contained in the Main Dolomite with the clay minerals of the underlying Stinking Shale might have contributed to the formation of the diasteranes. The suggestion of the authors about the migration of steranes from the T-2 bed into Ca2 bed is supported by the preservation of sesquiterpanes (less susceptible to degradation) in the A1g-3 (minor abundance), T2-1, T2-2, T2-3 (traces) and the Ca2-1 sample, where their concentration is the highest.

The preservation of steranes only in the Main Dolomite strata, where the accumulation of hydrocarbons within the dolomite-rich bed was greater than in the rock types both above and below it, results from their slower maturation, owing to

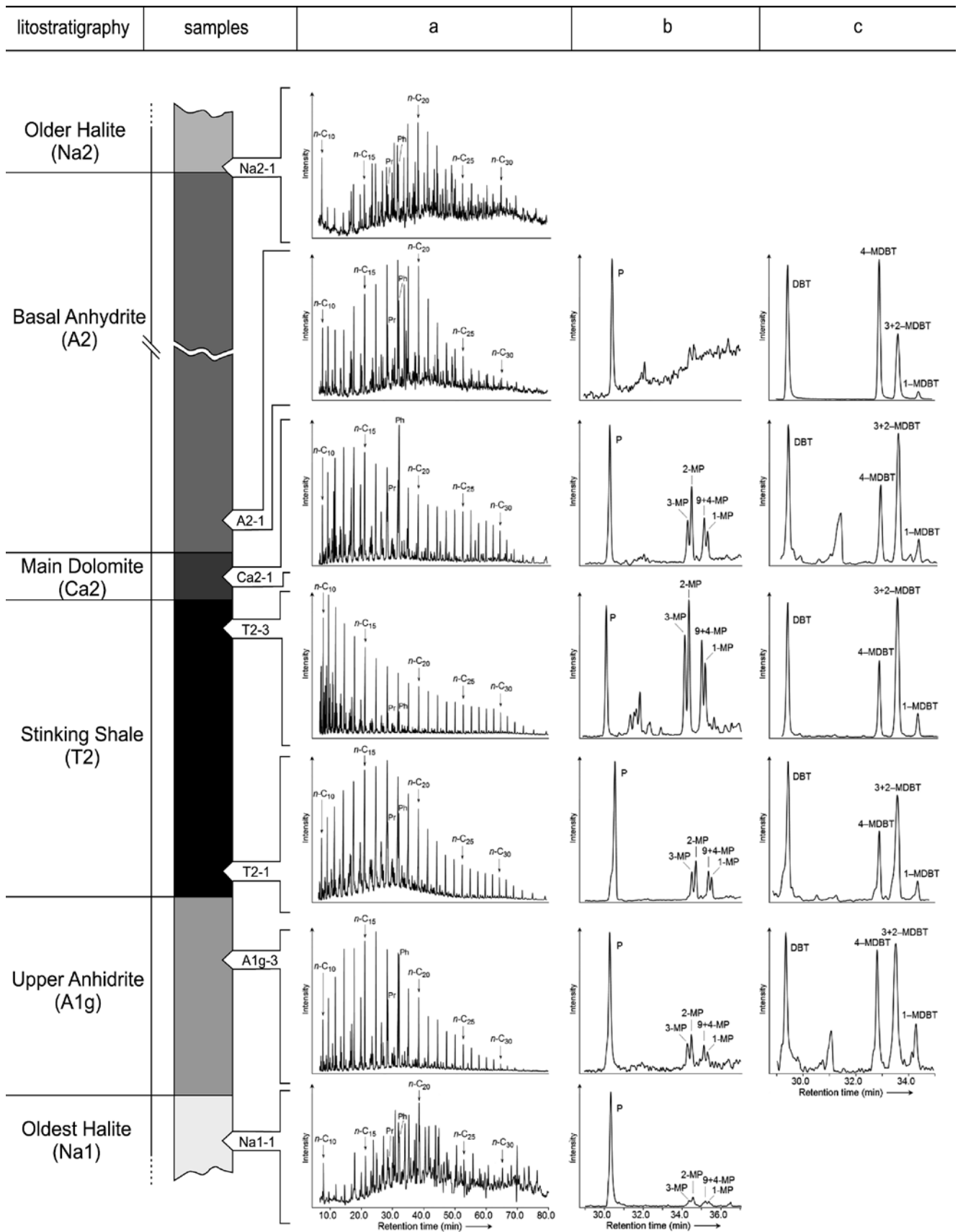


Fig. 3. Mass chromatograms (m/z 71) for n -alkanes – and acyclic isoprenoids (Pr – pristane, Ph – phytane) in column a; summed mass chromatograms (m/z 178 + 192) for phenanthrene (P) and methylphenanthrenes (MP) in column b; summed mass chromatograms (m/z 184 + 198) for dibenzothiophene (DBT) and methyl dibenzothiophenes (MDBT) in column c in extracts for selected samples from PZ1–PZ2 lithostratigraphic units of Klodawa Salt Structure.

the lesser influence of the mineral matrix on the rearrangement of the hydrocarbons. In other words, the greater concentration of hydrocarbons favoured their slower maturation.

The molecular composition of sterane homologues attained both optical and stereochemical equilibria (Fig. 4, trace A). The 20S/(20S+20R) ratio of C₂₉ααα epimers reached a value of 0.51, while the ratio of C₂₉αββ/(ααα+αββ) stereoisomers is 0.58. The high maturity of the hydrocarbons is reflected in the C₂₉ααα/C₂₉αββ ratio, which equals 0.92. These parameters locate maturity of the hydrocarbons in the Ca2-1 sample (dolomitic anhydrite) at advanced stage of the oil-window zone (Peters and Moldowan, 1993; Peters *et al.*, 2005). In this sample, supposed secosteranes are also present, as suggested by Kluska *et al.*, (2013). Their mass fragmentogram *m/z* 219 is shown in Fig. 4, trace B. However, the authors also observed methyl- and ethyl- derivatives of this series of compounds (Fig. 4, traces C – *m/z* 233 and D – *m/z* 247, respectively) with very similar chromatographic profiles, while derivatives of regular methyl- and ethylsteranes are not present. This lack of consistency may be an indication that the inferred secosteranes (Fig. 4, traces B, C and D) in fact represent different compounds, which so far were not identified.

Supporting information on the nature of the deposits during their sedimentation derives from the molecular signature of the *n*-alkylbenzenes, found in the Stinking Shale and Main Dolomite beds. Representative *m/z* = 92 mass fragmentograms for the T2-2 and Ca2-1 samples are shown in Fig. 5. Homologous distributions of *n*-alkylbenzenes are characterised by the prevalence of homologues with a lower molecular mass (below C₂₀). Their maximum abundance is centred on homologue C₁₅ in T2-1, T2-2 and Ca2-1 and shifts to a lower-molecular-mass homologue C₁₃ in the T2-3 sample. Higher molecular mass *n*-alkylbenzenes, with a less pronounced maximum centred at C₂₉, were observed in the Ca2-1 and the T2-1 samples. Their greater abundance, relative to counterparts with lower molecular mass in the Ca2-1 sample, is interpreted as being due to the upward migration of hydrocarbons from the underlying Stinking Shale, as was suggested for hydrocarbons accumulated in the Main Dolomite of Western Poland (Czechowski *et al.*, 1998). Homologous distribution of higher molecular mass *n*-alkylbenzenes differs in the prevalence of odd C₁₉, C₂₁ and C₂₃ over the even-carbon-numbered C₁₈, C₂₀, C₂₂ and C₂₄ *n*-alkylbenzenes in the Ca2-1 and the T2-1 samples (Fig. 5). This prevalence is clearly pronounced in the Ca2-1 sample, while it is lacking in the Stinking Shale samples. This distinguishing feature, observed in the Ca2-1 sample, indicates an association with the deposition of the source organic matter in the carbonate matrix and identifies the Ca2 horizon, in spite of the diagenetic anhydritization of the dolomite deposits.

Free carboxylic acids of low concentration and very similar homological composition were observed in the samples analysed, except for Ca2-1. A typical *m/z* 60 mass fragmentogram for the T2-1 sample is illustrated in Fig. 6. They are represented by a mixture of lower-molecular-weight homologous series of C₅ – C₉ *n*-alkanoic acids, where *n*-hexanoic acid dominates as well as by even-carbon-numbered *n*-fatty acids i.e. lauric (C₁₂ – dominant concentration), myristic (C₁₄), palmitic (C₁₆) and stearic (C₁₈) acids. Such a composition is typical for evaporites and can be related

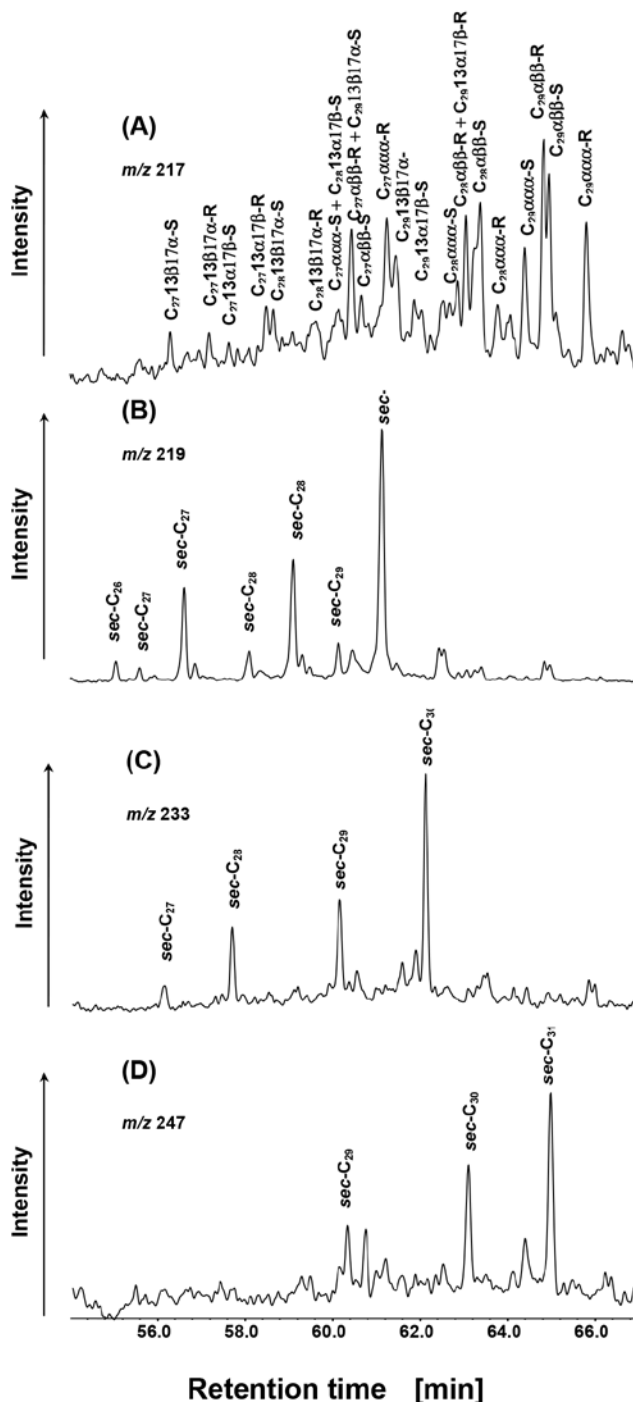


Fig. 4. Mass fragmentograms showing molecular distribution of steranes + diasteranes (A – *m/z* 217) and secosteranes (B – *m/z* 219, C – *m/z* 233, D – *m/z* 247) in Main Dolomite Ca2-1 sample.

to an algal source of the organic matter (Middelburg *et al.*, 1993; Volkman *et al.*, 1998).

Source, depositional environment and genetic type of organic matter

The isomeric composition of methylphenanthrenes can be source-dependent, with abundant 1-MP as indicative of a terrestrial origin and 9-MP for organic matter derived from

Table 1

Biomarker and aromatic compound parameters for samples of sulphate–shale–carbonate–sulphate series, separating PZ1 and PZ2 rock salt beds in the Kłodawa Salt Structure.

Parameter	Sample										
	Na1-1	A1g-1	A1g-2	A1g-3	T2-1	T2-2	T2-3	Ca2-1	A2-1	A2-2	Na2-1
<i>n</i> -Alkane of a highest abundance	<i>n</i> -C ₂₀	<i>n</i> -C ₁₈	<i>n</i> -C ₁₈	<i>n</i> -C ₁₆	<i>n</i> -C ₁₇	<i>n</i> -C ₁₅	<i>n</i> -C ₁₁	<i>n</i> -C ₁₃	<i>n</i> -C ₁₉	<i>n</i> -C ₂₀	<i>n</i> -C ₂₀
<i>n</i> -C ₂₁₋ / <i>n</i> -C ₂₁₊	—	1.64	2.33	4.92	6.68	8.26	4.22	3.06	3.50	—	—
Pr/ <i>n</i> -C ₁₇	1.09	2.25	1.33	0.86	0.44	0.34	0.41	0.70	1.16	1.47	1.30
Ph/ <i>n</i> -C ₁₈	1.12	2.60	1.94	1.37	0.92	0.98	0.47	1.81	1.02	1.29	1.58
Pr/Ph	0.85	0.66	0.63	0.67	0.73	0.75	1.17	0.43	1.09	0.90	0.89
CPI _(<i>n</i>-C₁₃–<i>n</i>-C₂₁)	—	0.89	0.73	0.90	1.02	0.95	0.96	0.904	0.95	—	—
CPI _(<i>n</i>-C₂₃–<i>n</i>-C₃₁)	—	1.31	1.21	1.06	1.01	1.05	0.97	0.94	1.15	—	—
TAR	—	0.55	0.26	0.09	0.07	0.08	0.25	0.21	0.14	—	—
% C ₂₇ -C ₂₈ -C ₂₉	—	—	—	—	—	—	—	18, 22, 60	—	—	—
C ₂₉ ααα20S/(20S + 20R)	—	—	—	—	—	—	—	0.51	—	—	—
C ₂₉ αββ/(ααα + αββ)	—	—	—	—	—	—	—	0.58	—	—	—
C ₂₉ ααα/C ₂₉ αββ	—	—	—	—	—	—	—	0.92	—	—	—
2-MP + 3-MP/1-MP + 9-MP	1.44	1.30	1.54	1.91	1.39	1.33	1.49	1.64	—	—	—
1-MP/9-MP	0.82	0.74	0.60	0.76	0.66	0.63	0.77	0.65	—	—	—
MPI-1	0.20	0.35	0.30	0.50	0.45	0.73	1.18	0.78	—	—	—
R _c [%]	0.52	0.61	0.58	0.70	0.67	0.84	1.11	0.87	—	—	—
MDR	—	—	—	3.84	3.36	3.29	3.11	3.55	18.36	—	—
DBT/P	0.14	0.32	0.29	0.71	0.61	1.28	2.48	0.89	7.97	0.10	0.05

Explanation: Carbon Preference Index for *n*-alkanes - CPI

$$CPI_{(n-C_{13} - n-C_{21})} = [n-C_{13} + 2(n-C_{15} + n-C_{17} + n-C_{19}) + n-C_{21}] / [2(n-C_{14} + n-C_{16} + n-C_{18} + n-C_{20})]$$

$$CPI_{(n-C_{23} - n-C_{31})} = [n-C_{23} + 2(n-C_{25} + n-C_{27} + n-C_{29}) + n-C_{31}] / [2(n-C_{24} + n-C_{26} + n-C_{28} + n-C_{30})]$$

$$n-C_{21-} / n-C_{22+} = \sum \leq n-C_{21} \text{ } n\text{-alkanes} / \sum \geq n-C_{22} \text{ homologues}$$

$$\text{Terrigenous/Aquatic Ratio: TAR} = [(n-C_{27} + n-C_{29} + n-C_{31}) / (n-C_{15} + n-C_{17} + n-C_{19})]$$

$$C_{29} \text{ } \alpha\alpha\alpha \text{ 20S} / (20S + 20R) = (\alpha\alpha\alpha 20S) / (\alpha\alpha\alpha 20S + \alpha\alpha\alpha 20R) \text{ of } C_{29} \text{ sterane}$$

$$C_{29} \text{ } \alpha\beta\beta / (\alpha\alpha\alpha + \alpha\beta\beta) = (\alpha\beta\beta 20R + \alpha\beta\beta 20S) / (\alpha\alpha\alpha 20S + \alpha\alpha\alpha 20R + \alpha\beta\beta 20R + \alpha\beta\beta 20S) \text{ of } C_{29} \text{ sterane}$$

$$C_{29} \text{ } \alpha\alpha\alpha / C_{29} \text{ } \alpha\beta\beta = (\alpha\alpha\alpha 20S + \alpha\alpha\alpha 20R) / (\alpha\beta\beta 20R + \alpha\beta\beta 20S) \text{ of } C_{29} \text{ sterane}$$

$$\text{Methylphenanthrene Index: MPI-1} = 1.5x(2\text{-MP} + 3\text{-MP}) / (P + 1\text{-MP} + 9\text{-MP})$$

$$\text{Calculated vitrinite reflectance: } R_c = 0.60x\text{MPI-1} + 0.40 \text{ } [\%]$$

$$\text{Methylphenanthrene ratio: MPR} = 2\text{-MP} / 1\text{-MP}$$

$$\text{Methyldibenzothiophene ratio: MDR} = 4\text{-MDBT} / 1\text{-MDBT}$$

a marine environment (Radke *et al.*, 1986; Budzinski *et al.*, 1995). The latter is also generated upon geosynthesis (Alexander *et al.*, 1995; Szczerba and Rospondek, 2010). The authors assumed that geosynthetic attribution of the 9-MP to methylphenanthrenes in the Permian rocks investigated is rather low and comparable for the corresponding lithofacies. The rocks derive from profile of one Permian cyclothem and underwent the same subsidence history. Therefore, the ratio of 1-MP/9-MP (Table 1) can be applied in identification of the source organic matter. In all rocks, the 1-MP/9-MP ratio value is below unity, which indicates marine organic matter. The indication of an origin as marine organic matter is supported by the great abundance of dibenzothiophene (DBT)

and methyldibenzothiophenes (MDBT) in all samples analysed (Fan *et al.*, 1990; Radke *et al.*, 2000), shown in Fig. 3, column c. Moreover, the observed predominance of short-over long-chain *n*-alkanes also may indicate the input of algal and/or bacterial biomass into the organic matter studied (Han and Calvin, 1969; Tissot *et al.*, 1977; Peters and Moldowan, 1993). The prevalence of even-carbon-numbered *n*-alkanes, observed in both rock salt samples (Na1-1 and Na2-1; Fig. 3), with *n*-C₂₀ the most abundant, reflects carboxylic group reduction in even-carbon-numbered fatty acids under anoxic hypersaline conditions. In these rock salts, β-carotane was also found and its presence is in accord with hypersaline conditions of formation.

Genetic type, depositional environment and thermal maturity of kerogen in the rocks were assessed from the ratios of $Pr/n-C_{17}$ vs. $Ph/n-C_{18}$ (Didyk *et al.*, 1978). The locations of the values of $Pr/n-C_{17}$ vs. $Ph/n-C_{18}$ are illustrated on diagrams by Obermajer *et al.* (1999) and Shanmugam (1985) in Fig. 7. In diagram A, data are located within the field for kerogen type II, typical of a marine environment, which confirms earlier findings by Czechowski *et al.*, 2011. Diagram B indicates algae and bacteria as the source of organic matter, which was preserved under reducing depositional conditions (Tissot and Welt, 1984). The Ca2 sediment was particularly rich in algal input and the corresponding point is located within the field of type I kerogen (Fig. 7A), with algal material as the main source (Fig. 7B). The location of points on the diagrams indicates the lowering of the maturity of hydrocarbons with distance from the T2-3 level. This is in accordance with the observations of Hoffmann and Leythaeuser (1995), who showed in their studies of boreholes in northern Germany, that pristane and phytane are expelled faster than $n-C_{17}$ and $n-C_{18}$ alkanes. Therefore, higher $Pr/n-C_{17}$ and $Ph/n-C_{18}$ ratios are to be expected for the earlier expelled hydrocarbons, together with a gradual lowering of them with progressive maturation in the direction of source rock.

Hydrocarbons maturity

To assess the maturity of hydrocarbons contained in the rocks a commonly accepted thermal maturity parameter, i.e., the Methyl Phenanthrene Index 1 (MPI-1), was used (Radke *et al.*, 1982; Radke and Welte, 1983). It is based on the abundances of phenanthrene and methylphenanthrenes and is explained with regard to the transformation of 1- and 9-methylphenanthrene isomers with lower thermal stability to the more thermodynamically stable 2- and 3- methylphenanthrenes during the course of hydrocarbons maturation; the MPI-1 equation is given in the footnote to Table 1. Mass chromatograms of the compounds (m/z 178 + 192) in the extracts from the rocks investigated are shown in Fig. 3, column b. In the Stinking Shale bed, at the depth of sample T2-3, similar concentrations of phenanthrene and respective methylphenanthrenes are present. A gradual increase in the amount of phenanthrene, relative to methylphenanthrenes, proceeds in both directions, up and down the stratigraphic sequence from the depth of sample T2-3. Simultaneously, the relative abundances of 2-MP + 3-MP with higher stability, compared to their 1-MP + 9-MP counterparts with lower thermodynamic stability, are higher in the lithological horizons underlying and overlying the Stinking Shale (see data in Table 1). This indicates different isomeric equilibria for the methylphenanthrenes, depending on the migration distance from the T2 horizon as well as on the organic matter dispersion in the mineral matrix of each lithofacies. The observed variations in methylphenanthrenes equilibria and the simultaneous increase of phenanthrene abundance in the directions noted can be explained as the geochromatographic effect of a smaller phenanthrene molecule, more susceptible to migration, than bigger molecules of methylphenanthrenes, through poorly permeable mineral matrices. In addition, the authors consider the

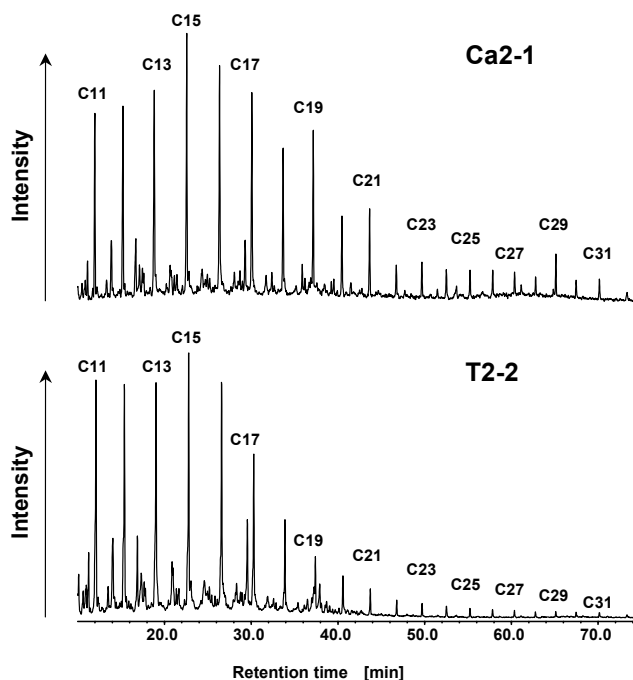


Fig. 5. Mass fragmentograms showing homological distribution of n -alkylbenzenes (m/z 92) in samples from Main Dolomite (Ca2-) and Stinking Shale (T2-2).

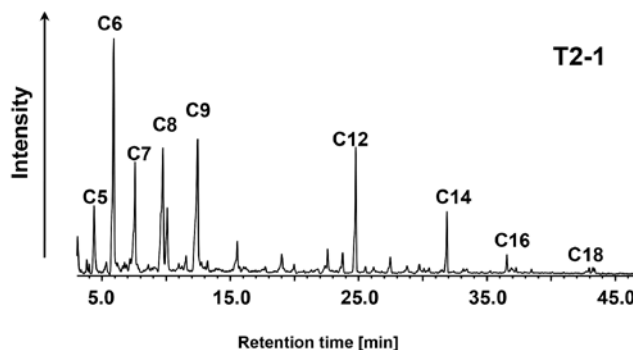


Fig. 6. Mass fragmentogram (m/z 60) showing molecular composition of free n -alkanoic acids in T2-1 sample.

possible demethylation of methylphenanthrenes expelled from the T2 horizon to generate more phenanthrene as well as their partial isomerization towards a more matured isomeric signature on a migration pathway in mineral matrices containing active sites, such as anhydrites. Supposition of migration distance and the role of the mineral matrix in the hydrocarbons transformation are additionally explained by a clearly noticeable isomerisation of methylthiophenes, the isomeric signature of which shows a progression in maturity along the migration pathways (Radke *et al.*, 1986; Alexander *et al.*, 1995; Asif *et al.*, 2009). This is reflected in the ratio increase of the 4- methylthiophene to 1- methylthiophene (mass chromatograms in Fig. 3, column c; data in Table 1).

The overall effect of these processes is averaged by values in formally calculated vitrinite reflectance (R_v) using

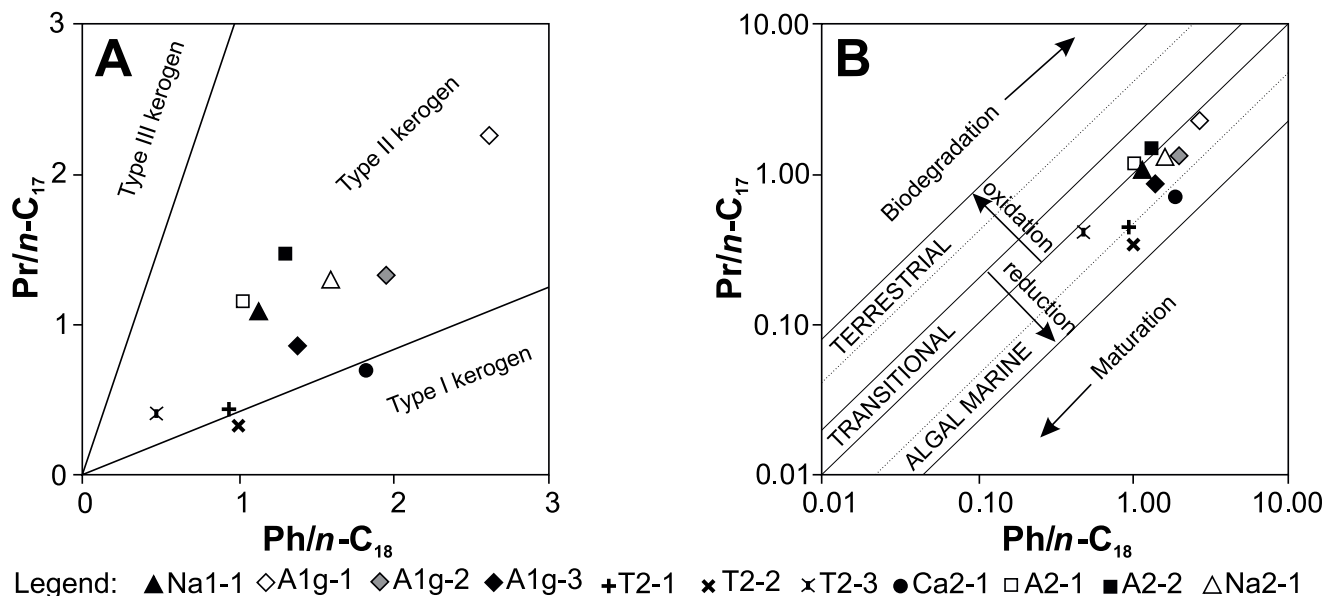


Fig. 7. Diagrams of $\text{Pr}/n\text{-C}_{17}$ vs. $\text{Ph}/n\text{-C}_{18}$, illustrating (A) kerogen type (after Obermajer *et al.*, 1999) and (B) source and depositional environment of organic matter (after Shanmugam, 1985).

the MPI-1 dependence defined by Radke and Welte (1983), as shown in Table 1. The R_c values cover a range of hydrocarbons maturity from an immature stage in the Na1-1 (R_c 0.52%) through the 'oil window' (stepwise from A1g-1 to T2-1) to end stage of the oil window (R_c 1.11%) for T2-3 (Radke and Welte, 1983; Peters *et al.*, 2005). In general, in spite of the critical consideration of the MPI-1 evaluation for hydrocarbons from the PZ1–PZ2 horizons analysed, these data support a trend of decreasing maturity of the hydrocarbons with increasing distance from the source rock – Fig. 8.

CONCLUSIONS

Insight is presented into the nature of the indigenous organic matter, contained in the PZ1–PZ2 rock sequence in the central part of the Polish Zechstein Basin and the organic

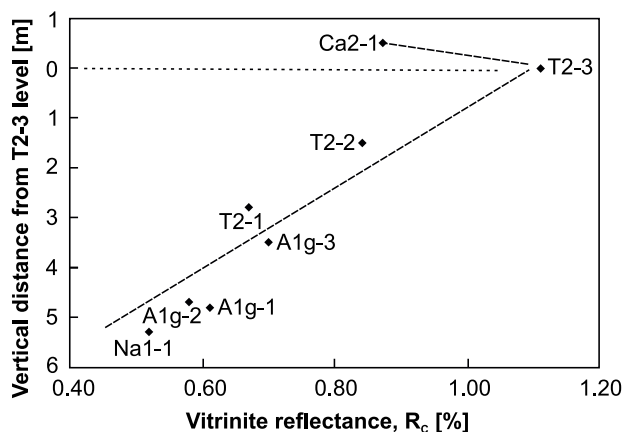


Fig. 8. Dependence of vitrinite reflectance R_c as function of vertical distance from depth of sample T2-3.

geochemical characteristics of the rocks. The organic matter in the rocks was isolated by rock salt from fluids circulating in the basin since the Triassic.

The organic matter was deposited under suboxic/anoxic environmental conditions in an organic-matter-poor and sulfur-rich marine environment. The major source rocks were the upper level of the Stinking Shale and the Main Dolomite beds. The kerogen is type II and of marine origin. Its maturity is at an advanced stage of the oil-window zone.

The source of the hydrocarbons contained in the PZ1–PZ2 rocks sequence was mainly algae, living in a marine environment. The molecular composition of hydrocarbons from the sulphate–shale–carbonate rock series, separating the PZ1 and PZ2 salt horizons in the KSS, is dominated by *n*-alkanes, *n*-alkylbenzenes, naphthalene and phenanthrene and their polymethyl derivatives. Dibenzothiophene and its polymethyl derivatives are present in smaller concentrations. Hopanoids are lacking, while steranes are preserved in small concentrations only in the Main Dolomite.

The hydrocarbons were expelled dominantly from the Stinking Shale horizon and migrated into both the overlying and underlying beds. Hydrocarbon maturity gradually decreases with increasing distance from the T2-3 sampling level, where the least matured hydrocarbons are at the greatest outermost distances, both upward and downward. This is in accord with the sequential generation and release of hydrocarbons, in which the first expelled and least mature ones migrated over the longest distance.

Acknowledgements

We are grateful to Piotr Krzywiec and Nykky Allen for their constructive comments that helped to considerably improve our manuscript. Mariusz Rospondek and Anonymous Reviewer helped in discussion on biomarkers.

REFERENCES

- Alexander, R., Bastow, T. P., Fisher, S. J. & Kagi, R. I., 1995. Geosynthesis of organic compounds: II. Methylation of phenanthrene and alkylphenanthrenes. *Geochimica et Cosmochimica Acta*, 59: 4259–4266.
- Asif, M., Alexander, R., Fazeelat, T. & Pierce, K., 2009. Geosynthesis of dibenzothiophene and alkyl dibenzothiophenes in crude oils and sediments by carbon catalysis. *Organic Geochemistry*, 40: 895–901.
- Bąkowski, J., 1986. Występowanie węglowodorów w strukturze solnej Kłodawy. *Zeszyty Naukowe Politechniki Śląskiej*, 140: 15–24. [In Polish.]
- Bąkowski, J. & Tokarski, A., 1966. Wschodnia ściana Kłodawy jako element naftowo-poszukiwawczy. *Zeszyty Naukowe AGH*, 139: 177–186. [In Polish.]
- Bourbonniere, R. A. & Meyers, P. A., 1996. Sedimentary geolipid records of historical changes in the watersheds and productivities of Lake Ontario and Erie. *Limnology and Oceanography*, 41: 352–359.
- Bray, E. E. & Evans, E. D., 1961. Distribution of *n*-paraffins as a clue to recognition of source beds. *Geochimica et Cosmochimica Acta*, 22: 2–15.
- Brooks, J. D., Gould, K. & Smith, J. W., 1969. Isoprenoid hydrocarbons in coal and petroleum. *Nature*, 222: 257–259.
- Budzinski, H., Garrigues, P., Connan, J., Devillers, J., Domine, D., Radke, M. & Oudins, J. L., 1995. Alkylated phenanthrene distributions as maturity and origin indicators in crude oils and rock extracts. *Geochimica et Cosmochimica Acta*, 59: 2043–2056.
- Burliga, S., 1996a. Implications for early basin dynamics of the Mid-Polish Trough from deformational structures within salt deposits in central Poland. *Geological Quarterly*, 40: 185–202.
- Burliga, S., 1996b. Kinematics within the Kłodawa salt diapir, central Poland. In: Alsop, G.I., Blundell, D. J. & Davidson, I. (eds), *Salt tectonics. Geological Society of London, Special Publication*, 100: 11–21.
- Burliga, S. & Czechowski, F., 2010. Anatomy of hydrocarbon-bearing zones, hydrocarbon provenance and their contribution to brittle fracturing of rock salt in the Kłodawa Salt Structure (central Poland). In: *Solution Mining Research Institute Spring 2010 Technical Conference*, Grand Junction, Colorado, USA pp. 125–134. [CD materials; no editor.]
- Burliga, S., Czechowski, F. & Hojniak, M., 2008. Gas hazards in the Kłodawa Salt Structure as a Zechstein stratigraphic indicator. *Mineral Resources Management*, 24: 69–81. [In Polish, with English summary.]
- Czechowski, F., Burliga, S. & Hojniak, M., 2011. Geochemistry of hydrocarbons from the first time documented occurrence of Main Dolomite (Ca₂) in the Kłodawa Salt Dome. *Geologia*, 37: 231–244. [In Polish, with English summary.]
- Czechowski, F., Piela, J., Grelowski, C., Hojniak, M., Wojtkowiak, Z. & Pikulski, L., 1998. Geochemical indications of continuity oil and gas basin in the Barnówko–Lubiszyn region (western Poland) as evidenced by the composition of liquid hydrocarbons in the Zechstein Main Dolomite. *Przeгляд Geologiczny*, 46: 171–177. [In Polish, with English summary.]
- Dadlez, R., 2003. Mesozoic thickness pattern in the Mid-Polish Trough. *Geological Quarterly*, 47: 223–240.
- Dadlez, R., Narkiewicz, M., Stephenson, R. A., Visser, M. T. M. & Van Wees, J.-D., 1995. Tectonic evolution of the Mid-Polish Trough: modelling implications and significance for central European geology. *Tectonophysics*, 252: 179–195.
- Didyk, C. B. M., Simoneit, B. R. T., Brassell, S. C. & Eglinton, G., 1978. Organic geochemical indicators of paleoenvironmental conditions of sedimentation. *Nature*, 272: 216–222.
- Fan, P., Philp, R.P., Zhenxi, L. & Guangguo, Y., 1990. Geochemical characteristics of aromatic hydrocarbons of crude oils and source rocks from different sedimentary environments. *Organic Geochemistry*, 16: 427–435.
- Han, J. & Calvin, M., 1969. Hydrocarbon distribution of algae and bacteria and microbial activity in sediments. *Proceedings of National Academy of Science USA*, 64: 436–443.
- Haven, H. L., ten, Leeuw, J. W. de & Schenck, P. A., 1985. Organic geochemical studies of a Messinian evaporitic basin, northern Apennines (Italy): I. Hydrocarbon biological markers for a hypersaline environment. *Geochimica et Cosmochimica Acta*, 49: 2181–2191.
- Haven, H. L., ten, Leeuw, J. W. de, Sinninghe Damste, J. S., Schenck, P. A., Palmer, S. E. & Zumberg, J., 1988. Application of biological markers in the recognition of palaeo-hypersaline environments. In: Fleet, A. J., Kelts, K. & Talbot, M. R. (eds), *Lacustrine Petroleum Source Rocks. Geological Society Special Publications*, 40: 123–130.
- Hofmann, P. & Leythaeuser, D., 1995. Migration of hydrocarbons in carbonate source rocks of the Staffurt member (Ca₂) of the Permian Zechstein, borehole Aue 1, Germany: the role of solution seams. *Organic Geochemistry*, 23: 597–606.
- Hunt, J. M., 1996. *Petroleum Geochemistry and Geology*, 2nd edition. W. H. Freeman and Co., New York, 743 pp.
- Jarosiński, M., Poprawa, P. & Ziegler, P. A., 2009. Cenozoic dynamic evolution of the Polish Platform. *Geological Quarterly*, 53: 3–26.
- Jaworowski, K. & Mikołajewski, M., 2007. Oil- and gas-bearing sediments of the Main Dolomite (Ca₂) in the Międzychód region: a depositional model and the problem of the boundary between the second and third depositional sequences in the Polish Zechstein Basin. *Przeгляд Geologiczny*, 55: 1017–1024.
- Karnkowski, P. H., 2007. Permian Basin as a main exploration target in Poland. *Przeгляд Geologiczny*, 55: 1003–1015.
- Kluska, B., Rospondek, M. J., Marynowski, L. & Schaeffer, P., 2013. The Werra cyclotheme (Upper Permian, Fore-Sudetic Monocline, Poland): Insights into fluctuations of the sedimentary environment from organic geochemical studies. *Applied Geochemistry*, 29: 73–91.
- Kotarba, M. J., Peryt, T., M., Kosakowski, P. & Więclaw, D., 2006. Organic geochemistry, depositional history and hydrocarbon generation modelling of the Upper Permian Kupferschiefer and Zechstein Limestone strata in south-west Poland. *Marine and Petroleum Geology*, 23: 371–386.
- Kotarba, M. & Wagner, R., 2007. Generation potential of the Zechstein Main Dolomite (Ca₂) carbonates in the Gorzów Wielkopolski–Międzychód–Lubiatów area, geological and geochemical approach to microbial–algal source rock. *Przeгляд Geologiczny*, 55: 1025–1036. [In Polish, with English summary.]
- Kovalevych, V. M., Peryt, T. M., Shanina, S. N., Więclaw, D. & Lytvyniuk, S. F., 2008. Geochemical aureoles around oil and

- gas accumulations in the Zechstein (upper Permian) of Poland: Analysis of fluid inclusions in halite and bitumens in rock salt. *Journal of Petroleum Geology*, 31: 245–262.
- Krzywiec, P., 2004. Triassic evolution of the Kłodawa salt structure: basement-controlled salt tectonics within the Mid-Polish Trough (Central Poland). *Geological Quarterly*, 48: 123–134.
- Krzywiec, P., 2006a. Structural inversion of the Pomeranian and Kuiavian segments of the Mid-Polish Trough – lateral variations in timing and structural style. *Geological Quarterly*, 51: 151–168.
- Krzywiec, P., 2006b. Triassic–Jurassic evolution of the Pomeranian segment of the Mid-Polish Trough—basement tectonics and subsidence patterns. *Geological Quarterly*, 50: 139–150.
- Krzywiec, P., Gutowski, J., Walaszczyk, I., Wróbel, G. & Wybraniec, S., 2009. Tectonostratigraphic model of the Late Cretaceous inversion along the Nowe Miasto – Zawichost fault zone, SE Mid-Polish Trough. *Geological Quarterly*, 53: 27–48.
- Kucia, Z., 1970. Nowe człony stratygraficzne cechsztynu w kopalni „Kłodawa”. *Przegląd Geologiczny*, 18: 345–346. [In Polish.]
- Middelburg, J. J., Baas, M., ten Haven, H. L. & de Leeuw, J. W., 1993. Organic geochemical characteristics of sediments from Kau Bay. In: Oygard, K. (ed.), *Organic Geochemistry: Poster Sessions from the 16th International Meeting on Organic Geochemistry*, Stavanger. Falch Hurtigtrykk, Oslo, pp. 413–417.
- Misiek, G., 1997. Stratygrafia i wykształcenie utworów cechsztynu w wysadzie solnym Kłodawy. In: Burliga, S. (ed.), *Salt Tectonics in the Kuiavian Region*. Proceedings of the conference on Salt Tectonics in the Kuiavian Region. WIND, Wrocław, pp. 20–23.
- Natkaniec-Nowak, L., Heflik, W., Pawlikowski, M. & Sikora, M., 2001. Petrochemical studiem of bitumic salts from PZ2 horizon (Kłodawa Salt Mine). *Geologia*, 27: 383–407.
- Obermajer, M., Fowler, M. G. & Snowdon, L. R., 1999. Depositional environment and oil generation in Ordovician source rocks from southwestern Ontario, Canada: Organic geochemical and petrological approach. *AAPG Bulletin*, 83: 1426–1453.
- Peryt, T. M., Geluk, M. C., Mathiesen, A., Paul, J. & Smith, K., 2010. Zechstein. In: Doornenbal, J. C. & Stevenson, A. G. (eds), *Petroleum Geological Atlas of the Southern Permian Basin Area*. EAGE Publications b.v., Houten, pp. 123–147.
- Peryt, T. M. & Wagner, R., 1998. Zechstein evaporite deposition in the Central European Basin: cycles and stratigraphic sequences. *Journal of Seismic Exploration*, 7: 201–218.
- Peters, K. E. & Moldowan, J. M., 1993. *The Biomarker Guide: Interpreting Molecular Fossils in Petroleum and Ancient Sediments*. Prentice–Hall, New Jersey, 363 pp.
- Peters, K. E., Walters, C. C. & Moldowan, J. M., 2005. *The Biomarker Guide, 2nd Edition: Volume 2 Biomarkers and Isotopes in Petroleum Systems and Earth History*. Cambridge University Press, Cambridge, 679 pp.
- Powell, T. G. & McKirdy, D. M., 1973. Relationship between ratio of pristane to phytane, crude oil composition and geological environment in Australia. *Nature Physical Science*, 243: 37–39.
- Radke, M., Vriend, S. P. & Ramanampisoa, L. R., 2000. Alkyldibenzofurans in terrestrial rocks: influence of organic facies and maturation. *Geochimica et Cosmochimica Acta*, 64: 275–286.
- Radke, M. & Welte, D. H., 1983. The methylphenanthrene index (MPI): a maturity parameter based on aromatic hydrocarbons. In: Bjorøy, M., Albrecht, P., Cornford, C., de Groot, K., Eglinton, G., Galimov, E., Leythaeuser, D., Pelet, R., Rullkötter, J. & Speers, G. (eds), *Advances in Organic Geochemistry 1981*. Wiley, Chichester, pp. 504–512.
- Radke, M., Welte, D. H. & Willsch, H., 1982. Geochemical study on a well in the Western Canada Basin: relation of the aromatic distribution pattern to maturity of organic matter. *Geochimica et Cosmochimica Acta*, 46: 1–10.
- Radke, M., Welte, D. H. & Willsch, H., 1986. Maturity parameters based on aromatic hydrocarbons: influence of the organic matter type. *Organic Geochemistry*, 10: 51–63.
- Sarg, J. F., 2001. The sequence stratigraphy, sedimentology, and economic importance of evaporite–carbonate transitions: a review. *Sedimentary Geology*, 140: 9–42.
- Shanmugam, G., 1985. Significance of coniferous rain forests and related organic matter in generating commercial quantities of oil, Gippsland Basin, Australia. *AAPG Bulletin*, 69: 1241–1254.
- Słowakiewicz, M. & Mikołajewski, Z., 2009. Sequence stratigraphy of the upper Permian Zechstein Main Dolomite carbonates in western Poland: a new approach. *Journal of Petroleum Geology*, 32: 215–234.
- Słowakiewicz, M. & Mikołajewski, Z., 2011. Upper Permian Main Dolomite microbial carbonates as potential source rocks for hydrocarbons (W Poland). *Marine and Petroleum Geology*, 28: 1572–1591.
- Szczerba, M. & Rospondek, M. J., 2010. Controls on distributions of methylphenanthrenes in sedimentary rock extracts: critical evaluation of existing geochemical data from molecular modelling. *Organic Geochemistry*, 41: 1297–1311.
- Tissot, B. P., Pelet, R., Roucache, J. & Combaz, A., 1977. Alkanes as geochemical fossils indicators of geological environments. In: Campos, R. & Goni, J. (eds), *Advances in Organic Geochemistry 1975*. Enadimsa, Madrid, pp. 117–154.
- Tissot, B. P. & Welt, D. H., 1984. *Petroleum Formation and Occurrence*. Springer, Berlin Heidelberg, 699 pp.
- Toboła, T., 2010. Inclusions in bituminous salts from Kłodawa Salt Dome. *Geologia*, 36: 345–365. [In Polish, with English summary.]
- Volkman, J. K., 1986. A review of sterol markers for marine and terrigenous organic matter. *Organic Geochemistry*, 9: 83–99.
- Volkman, J. K., Barrett, S. M., Blackburn, S. I., Mansour, M. P., Sikes, E. L. & Gelin, F., 1998. Microalgal biomarkers: A review of recent research developments. *Organic Geochemistry*, 29: 1163–1179.
- Wagner, R., 1994. Stratigraphy of deposits and development of Zechstein Basin in Polish Lowlands. *Prace Państwowego Instytutu Geologicznego*, 146: 5–62. [In Polish, with English summary.]
- Wagner, M. & Burliga, S., 2014. Coalified bitumens from the Kłodawa Salt Structure (central Poland) as evidence on migration of hydrothermal fluids in Zechstein (Upper Permian) deposits. *Geological Quarterly*, 58: 545–554.
- Warren, J., 1999. *Evaporites. Their Evolution and Economics*. Blackwell Science Ltd., Oxford, 438 pp.
- Ziegler, P. A., 1990. *Geological Atlas of Central and Western Europe, Second edition*. Shell Internationale Petroleum Maatschappij B. V., Geological Society Publishing House, Bath, 256 pp.